

Monitoring of carbon dioxide and water vapour exchange over a young mixed forest plantation using eddy covariance technique

T. Watham^{1,*}, S. P. S. Kushwaha¹, N. R. Patel¹ and V. K. Dadhwal²

¹Indian Institute of Remote Sensing, ISRO, Dehradun 248 001, India

²National Remote Sensing Centre, ISRO, Hyderabad 500 625, India

Studies on CO₂ and water vapour exchange in natural and man-made vegetation are necessary for quantifying their role in landscape-level carbon budget. The present study investigated variations in carbon and water vapour fluxes and monthly net ecosystem exchange (NEE) over a 9-year-old mixed forest plantation (*Holoptelea integrifolia*, *Dalbergia sissoo*, *Acacia catechu* and *Albizia procera*) in Terai Central Forest Division of Nainital district, Uttarakhand using January to September 2013 eddy covariance data. During leafless period (i.e. January), the plantation acted as a net carbon source (i.e. positive NEE) with daily mean release of 0.35 g C m⁻² day⁻¹, while from leaf onset to growing period (i.e. April to September), it acted as a sink (i.e. negative NEE) due to carbon uptake by an increasing number of leaves. The monthly mean daily NEE was noticed to be increasingly more negative in each subsequent month until September. The diurnal trend in NEE closely followed the variations in the intensity of photosynthetically active radiation. The diurnal NEE in all months was related to vapour pressure deficit with time-lag. Maximum daytime uptake (−29.5 μmol m⁻² s⁻¹) and night-time release of CO₂ (8.2 μmol m⁻² s⁻¹) was observed in July. Monthly mean of daily NEE over plantation continuously increased from February and was highest (−5.74 g C m⁻² day⁻¹) in September. Rectangular hyperbolic function provided reasonably good fit between NEE and PAR. Ecosystem parameters (α and P_{max}) of the light response curve also followed the canopy development trend.

Keywords: Carbon dioxide, eddy covariance, mixed forest plantation, water vapour.

CARBON, the building block of life, accounts for nearly half of the total dry mass of all living things¹. India, with its monsoon-based climate system, varied topography and diverse land use/land cover coupled with a variety of cultural practices, supports a vast mosaic of ecosystems with carbon sink and source capabilities. The agricultural and forest ecosystems, which cover ca. 180 mha and 68 mha respectively, contribute largely to terrestrial carbon dynamics in the country². Carbon dioxide (CO₂) is an important greenhouse gas (GHG) contributing to global

warming. The global concentration of CO₂ in the atmosphere is steadily increasing, largely as a result of human activities such as the burning of fossil fuel and biomass³. Accurate quantification of carbon fluxes of any ecosystem, region, continent or globe is necessary for understanding the feedback mechanism between terrestrial biosphere and the atmosphere. It also helps in making policy-oriented decisions on mitigating the global warming. Efforts to alleviate global warming by terrestrial carbon sequestration have paved the way for continuous research on more accurate quantification of terrestrial carbon sources and sinks⁴. Several techniques have been developed over the years to estimate the net exchange of CO₂ across terrestrial ecosystems–atmosphere boundary layer, including inventory approaches⁵, ecosystem modelling⁶ and atmospheric inverse modelling⁷. Approaches used to identify the nature of terrestrial carbon sources and sinks include direct flux tower-based measurements using eddy covariance methods⁸, analysis of forest inventory records⁹ and integration of historic land-use records within biogeochemical models¹⁰.

Among the established micrometeorological instrumentation techniques, the eddy covariance (EC) flux towers have been extensively used in the measurement of energy and mass exchange over forest, crop and grassland canopies to enhance our understanding of soil–vegetation–atmosphere carbon exchanges^{11–14}. The EC technique, a direct method of recording the ecosystem-level greenhouse gas fluxes, has been found to be a promising and effective means of measuring the exchange of CO₂ and water vapour fluxes on various spatial and temporal scales¹⁵. The technique measures exchange of CO₂ or water vapour as a product of vertical wind velocity and fluctuations in the molar concentration of CO₂ or H₂O. The uniqueness of the EC technique is that it can support measurement of CO₂ and H₂O fluxes at sub-diurnal to annual timescale and over an individual crop field to forest landscape^{16,17}.

Long-term tower-based EC method has been well-established worldwide, covering all major plant functional types and climates to monitor the terrestrial ecosystem–atmosphere exchange of GHGs, water vapour, and momentum and heat. Under FLUXNET, a global network formed by the combination of AMERIFLUX, CARBOEURO FLUX, ASIAFLUX, OZFLUX and other non-network sites, more than 547 flux towers have been installed worldwide till date. This network has been a great source of basic information about net CO₂ flux as the instrumentation can be maintained at any location for continuous measurements over several years. Most towers, however, are confined in the northern hemisphere mid-latitude locations with poor representation of tropical forests, despite being a major player in the global carbon and water cycle¹⁸. Early effort to identify the need and approach for developing flux network in India was made by Sundareshwar *et al.*¹⁹. According to Xiao *et al.*²⁰, a

*For correspondence. (e-mail: taibang01@gmail.com)

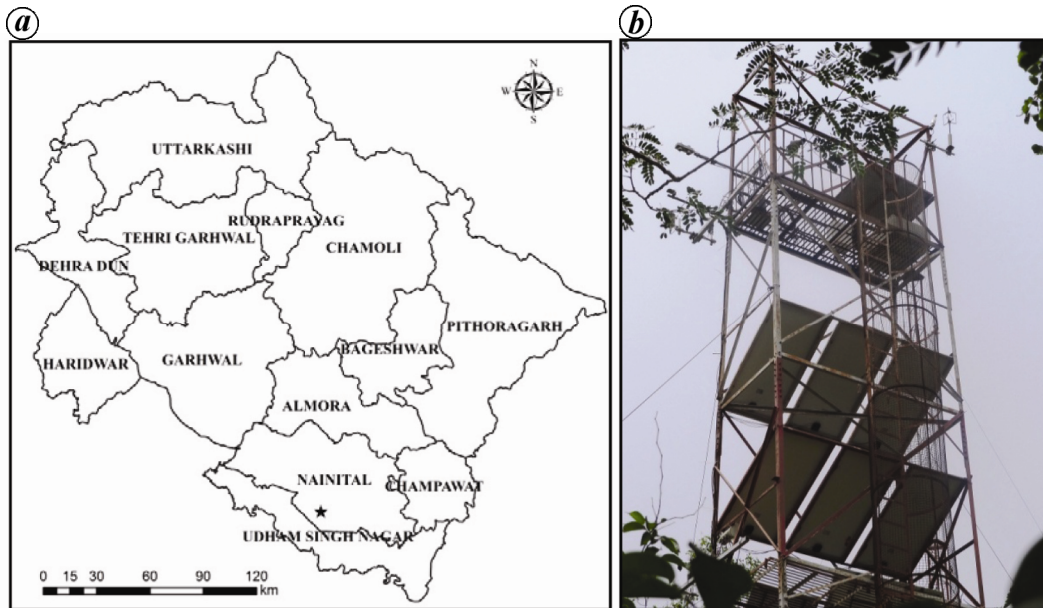


Figure 1. *a*, Location of the study site denoted by star. *b*, Haldwani flux tower.

combination of EC flux data and the upscaling technique can provide an alternative and independent approach to quantify the carbon and water exchange between the terrestrial biosphere and atmosphere from local to global scales.

The purpose of this study was to develop a better understanding of monthly variation of NEE in a young mixed forest plantation, and most importantly, to promote Indian tower-based CO₂ flux monitoring by sharing of our site knowledge among the researchers working on tower-based flux measurements, leading to the development of a fully functional INDOFLUX network.

The Haldwani flux site (29°8'57.55"N, 79°25'15.97"E, 280 m amsl) is situated in the Uttarakhand terai area southwest of Haldwani in Nainital district, Uttarakhand. The EC tower is located at the centre of plot number 27 covering an area of 44 ha (Figure 1). The plantation was raised by sowing the seeds of four deciduous forest species, viz. *Holoptelea integrifolia*, *Dalbergia sissoo*, *Acacia catechu* and *Albizia procera* in 2004 on very fertile land and the rate of growth has been fast since then. At present, the average tree height is 10 m. The undergrowth comprises of *Lantana camara*, *Clerodendrum viscosum* and *Parthenium hysterophorus*. The area receives 1500 mm mean annual rainfall with monsoon starting from middle of June and continuing until September. The heaviest rainfall occurs during July and August. Soil type is clayey to sandy loam, with pH ranging from 5.5 to 6.0 (ref. 21).

Various fast and slow EC and micrometeorological instruments were installed at 19 m height (9 m above canopy) and integrated in October 2012. EC data collected between January and September 2013 were used. A LI-COR (Lincoln, NE) LI-7500 open path infrared gas

analyser (IRGA) was used for measuring the CO₂ and H₂O mixing ratio at 10 Hz and a WindMaster 3D sonic anemometer (Gill Instruments Ltd, England) for measuring wind speed, wind direction and sonic temperature. In addition to the flux measurements, various micrometeorological parameters such as net radiation, air temperature, humidity, wind speed, wind direction, precipitation, barometric pressure, soil moisture and temperature at different depths were also recorded half-hourly. All flux and meteorological data were stored in compact flash card using data logger CR-3000 (Campbell Scientific, USA). All data were downloaded at 20-day intervals. At the top of the tower a Phenocam camera (CC5MPX, Campbell Scientific, USA) was used for accurate monitoring of vegetation phenology. Table 1 shows the specifications of various slow sensors and their height and depth from ground level.

Fluxes of CO₂, H₂O and energy are a function of varying concentration of CO₂ and H₂O, temperature and three-dimensional vectors of wind. Fluxes were calculated at half-hourly intervals by EC method. The raw data were collected and split in 30 min file using PC200W (Campbell Scientific, USA) software. After converting into ASCII format, data were analysed using EddyPro 4.1 (LI-COR, Lincoln, NE) software. The flux calculation was done as described by Burba²².

One intrinsic problem associated with EC measurement system is unreliability or unavailability of data during rain, snowfall and night due to weak turbulence^{23,24}. The problem of data gap in the present study occurred mainly due to power failure, primarily due to rainfall and fog. Some other minor problems included instrument failure and the integration of new instrument. For night-time filter, frictional velocity (u^*) value was set at 0.1 m/s. The

Table 1. Slow sensors for meteorological measurement

Observed parameters	Level/depth	Instrument
Shortwave radiation (incoming)	15 m	CNR1 Net radiometer (Kipp & Zonen)
Shortwave radiation (outgoing)	15 m	CNR1 Net radiometer (Kipp & Zonen)
Longwave radiation (incoming)	15 m	CNR1 Net radiometer (Kipp & Zonen)
Longwave radiation (outgoing)	15 m	CNR1 Net radiometer (Kipp & Zonen)
Net radiation	15 m	CNR1 Net radiometer (Kipp & Zonen)
Air temperature	5, 10, 15 m	HMP50 (Vaisala, Finland)
Humidity	5, 10, 15 m	HMP50 (Vaisala, Finland)
Soil temperature	5, 15, 30, 60 cm	Komoline (India)
Soil water content	5, 15, 30, 60 cm	Komoline (India)
Wind speed	5, 10, 15 m	Wind Monitor-05103 (R.M. Young)
Wind direction	5, 10, 15 m	Wind Monitor-05103 (R.M. Young)
Barometric pressure	15 m	PTB110 Barometer (Vaisala, Finland)
Phenocam	15 m	CC5MPX (Campbell Scientific)

Max Planck Institute of Biogeochemistry online service (<http://www.bgc-ena.mpg.de/~MDI/work/eddyproc/upload.php>), which follows methods similar to Falge *et al.*²⁵, but considers both co-variation of fluxes with meteorological variables and the temporal auto-correlation of fluxes²⁶, was used for data gap filling.

The study site remained leafless in January and a major part of February. By the end of February and the beginning of March, leaf development started. Young, tender, light-green leaves were formed by mid-April, which attained maturity by end of May. During June and July, the crown density remained more or less the same. Increase in the leaf density took place in August and dense canopy cover was formed by August end. The mean monthly air temperature (Temp_air) at 10 m height rose constantly from 8.95°C (in January) to 37.88°C (in May) with intermediate values of 13.54°C (February), 15.86°C (March), 21.01°C (April), 24.33°C (May), 27.99°C (June), 27.92°C (July), 27.34°C (August) and 26.51°C (September). The soil temperature (Temp_soil) followed similar trends. The mean diurnal variations in Temp_air and Temp_soil are shown in Figure 2 *a* and *c* respectively.

Measured relative air humidity (Rh_air) at 10 m above-ground showed a decreasing trend from February to May; from May onwards it started increasing. The mean diurnal monthly variations of Rh_air and soil moisture percentage are given in Figure 2 *b* and *d* respectively. During the study period, the Indian monsoon was slightly delayed compared to previous years. It started by end of June and continued till September. Heaviest rainfall was observed in July and August. The daily mean monthly photosynthetically active radiation (PAR) density ranged from 302.784 to 492.159 $\mu\text{mol m}^{-2} \text{s}^{-1}$. Minimum and maximum PAR density was observed in January and April respectively.

One of the accepted important tests for EC data is energy balance closure^{27–29}. Many FLUXNET studies^{30–32} have reported the energy balance closure as a standard procedure. Energy balance closure evaluation is useful in understanding the close biophysical coupling between

carbon, energy and water fluxes^{14,33}. Energy balance closure, a formulation of the first law of thermodynamics, requires that the sum of the estimated latent (LE) and sensible (*H*) heat flux be equivalent to all other energy sinks and sources

$$\text{LE} + H = R_n - G - S - Q, \quad (1)$$

where R_n is the net radiation, G the heat flux into the soil substrate, S the rate of change of heat storage (air and biomass) between the soil surface and the level of the EC instrumentation, and Q is the sum of all additional energy sources and sinks. Typically, Q is neglected as a small term and an imbalance between the remaining independently measured terms on the left- and right-hand sides of eq. (1) may indicate inaccurate estimates of scalar fluxes. Even under ideal conditions for the EC method, many authors have reported frequent underestimated surface energy fluxes by about 10–30% relative to estimates of available energy ($R_n - G - S$)^{29,34,35}. In the present study, an attempt to address energy closure balance was made using only LE, H and R_n . The measured R_n was compared against the calculated surface energy fluxes obtained from EC. The percentage deficit in the energy balance is shown in Table 2, excluding G and S . It ranged from 18.08% to 37.17%, which is acceptable as the value will come down below 30% when G and S are included.

Partitioning of the incoming radiation into LE and H fluxes is presented in Figure 3. It was observed that the incoming radiation was mostly used for heating the air during January and February, i.e. $H > \text{LE}$, which could be attributed to the leafless condition of the vegetation. From March, a gradual reversal in the H and LE values was noticed. The LE value was slightly higher than the H value in March, which signifies early phase of leaf development. During subsequent months, the gap between LE and H values became more pronounced due to increase in the leaf density.

Diurnal variation in net ecosystem exchange (NEE) was further partitioned into uptake, release and net daily

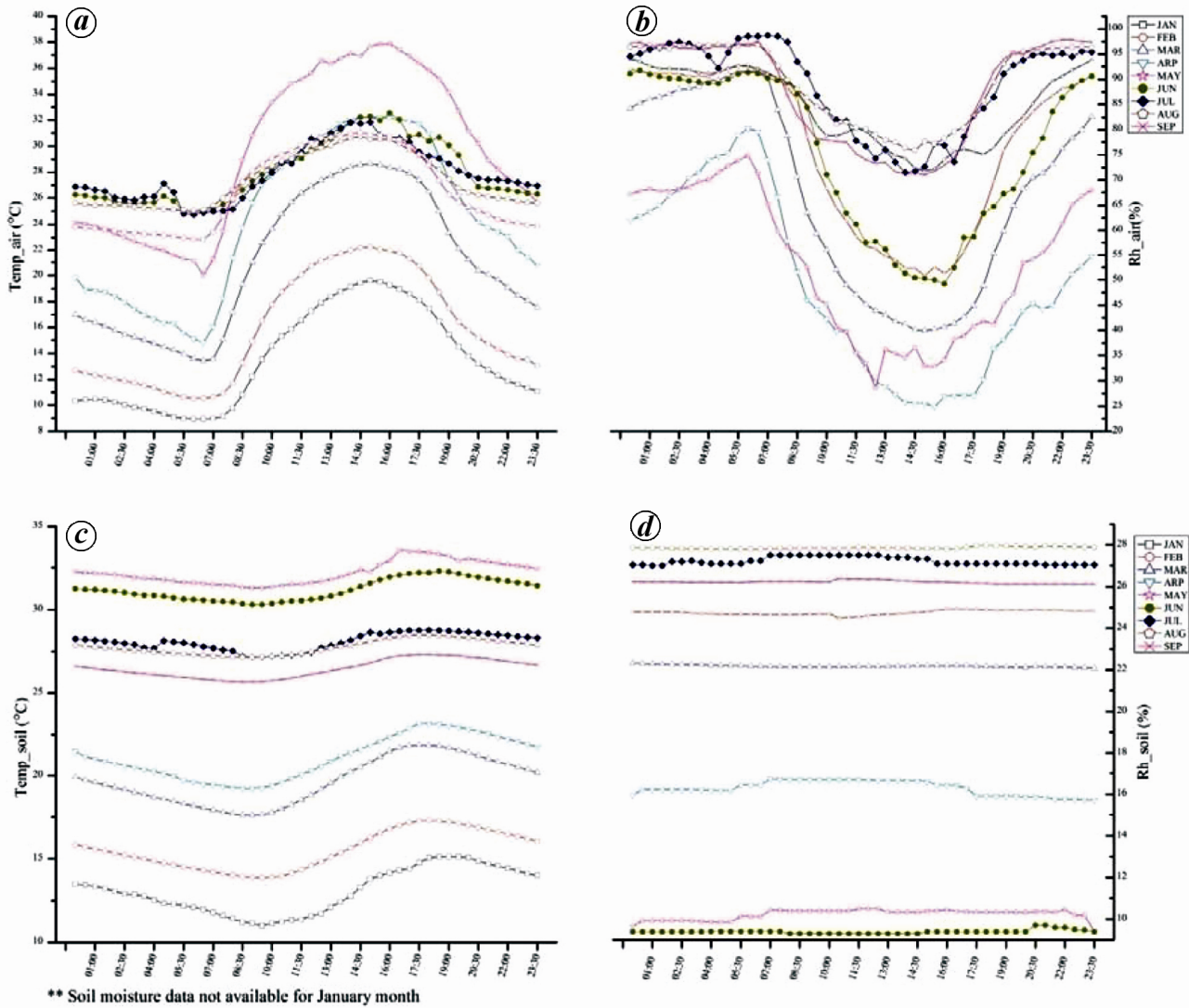


Figure 2. a, Mean monthly diurnal air temperature. b, Mean monthly diurnal relative air humidity. c, Mean monthly diurnal soil temperature. d, Mean monthly diurnal soil moisture.

Table 2. Monthly energy flux and deficit in energy balance

Month	R_n	LE	H	LE + H	Deficit (%)
January	119.8	29.85	54.21	84.07	29.82
February	148.54	43.08	59.33	102.41	31.05
March	211.27	83.85	48.86	132.72	37.17
April	237.58	132.49	35.57	168.07	29.25
May	191.6	105.9	45.96	151.86	20.74
June	157.08	84.35	44.31	128.67	18.08
July	160.8	113.83	12.03	125.86	21.72
August	177.01	106.08	12.93	119.02	32.75
September	204.68	114.91	14.27	129.19	36.88

R_n , Net radiation; LE, Latent heat; H, Sensible heat.

mean NEE for all months across the growing season of the forest plantation (Figure 4a and b). Negative and positive signs of NEE represent uptake by canopy and release of CO₂ to the atmosphere respectively. Diurnally,

the daytime uptake of CO₂ was more prominent during all months and generally followed the course of the movement of the Sun. The observed value of the daily NEE in January (+0.35 g C m⁻² day⁻¹) showed that the plantation acted as a source of carbon due to low uptake and more respiration from exposed (due to absence of vegetation canopy) soil, branches and twigs of tree species. Daytime uptake and night-time release of CO₂ started increasing from February and attained a peak value of -8.13 and 2.61 g C m⁻² day⁻¹ respectively, in August. However, daily total NEE followed a similar trend till September. The continuous increase in NEE values over the growing season reveals predominance of photosynthetic activity by increased leaf growth and leaf density/crown cover, thus leading to higher assimilation of carbon by the trees. The lowest value of daily mean NEE in February (-0.38 g C m⁻² day⁻¹) among all months could be ascribed to low photosynthetic rate from shoot than canopy³⁶.

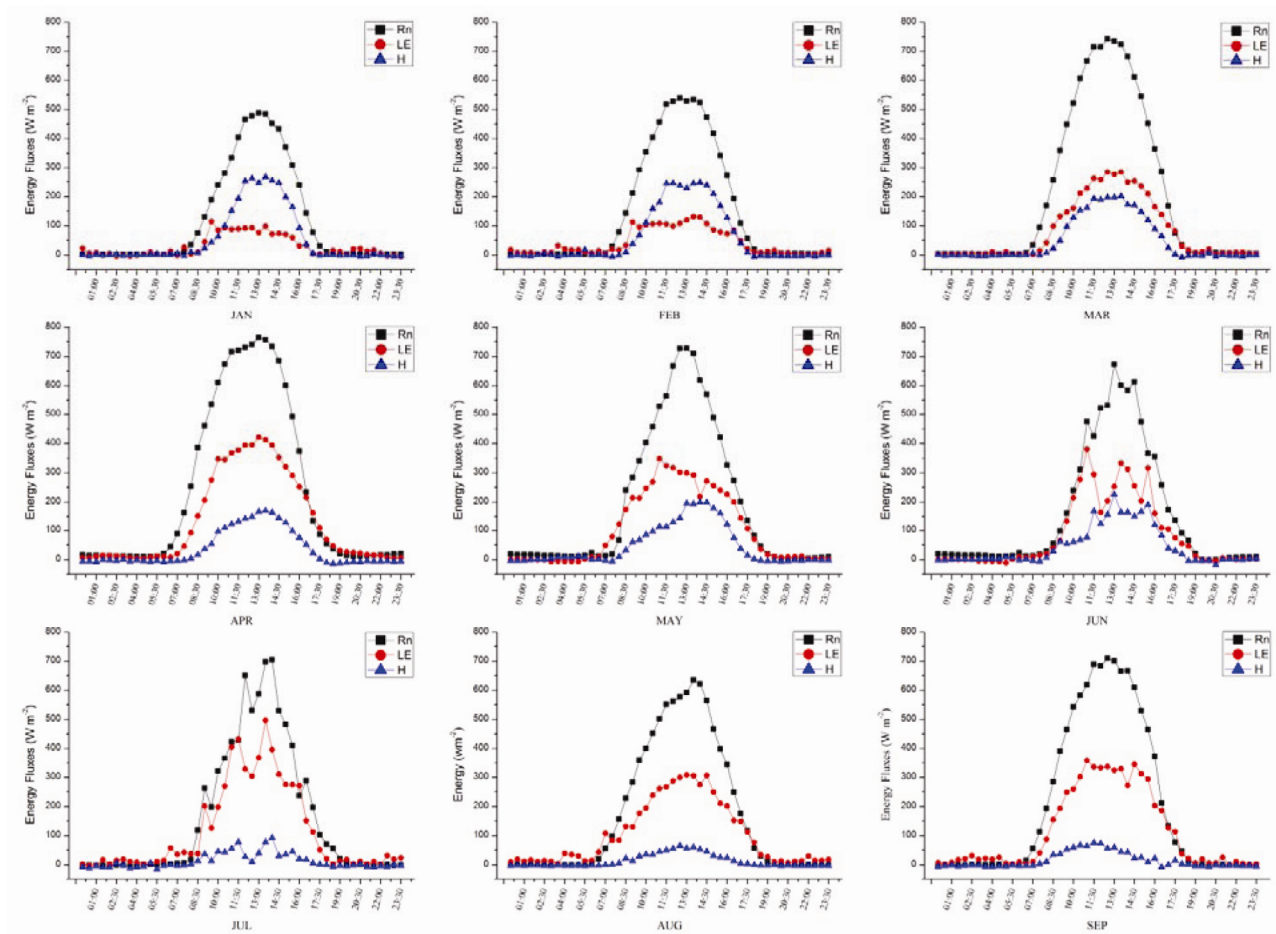


Figure 3. Partitioning of mean monthly diurnal net radiation (R_n) into sensible heat (H) and latent heat (LE).

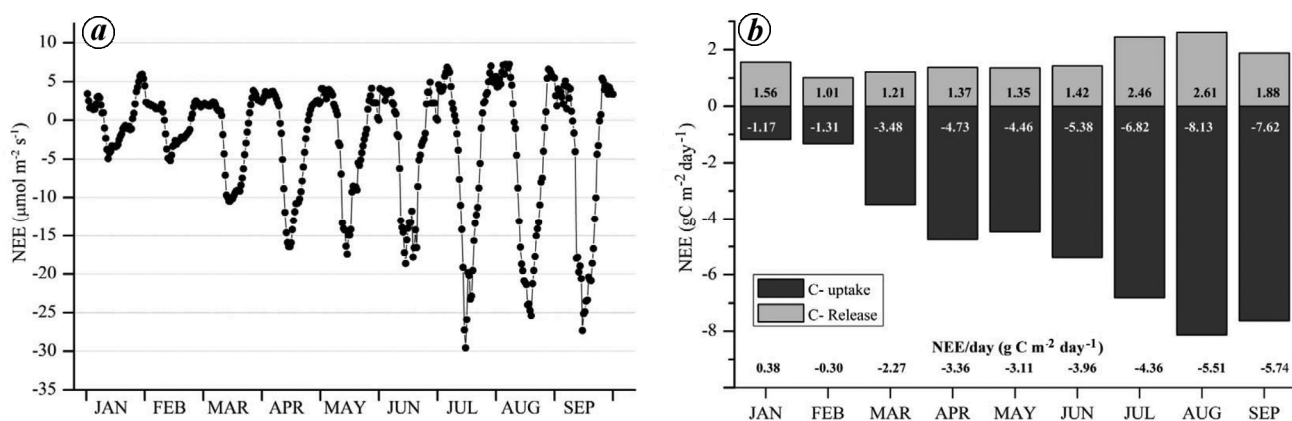


Figure 4. Mean monthly diurnal net ecosystem exchange (NEE) variation (a) and mean monthly daily NEE budget (b).

The highest magnitude of total daily NEE was $-5.74 \text{ g C m}^{-2} \text{ day}^{-1}$. The NEE value reported in the present study is slightly higher than that ($2\text{--}4 \text{ g C m}^{-2} \text{ day}^{-1}$) reported by Haszpra *et al.*³⁷ for mixed vegetation. A higher NEE value is expected in future when the canopy develops further.

The high-frequency diurnal variation in NEE (Gross primary productivity (GPP) minus ecosystem respiration, R_e) over mixed plantation followed the course of intensity of photosynthetically active radiation. Figure 5 represents the mean monthly diurnal variation in NEE with mean monthly variation in PAR. In general, NEE became

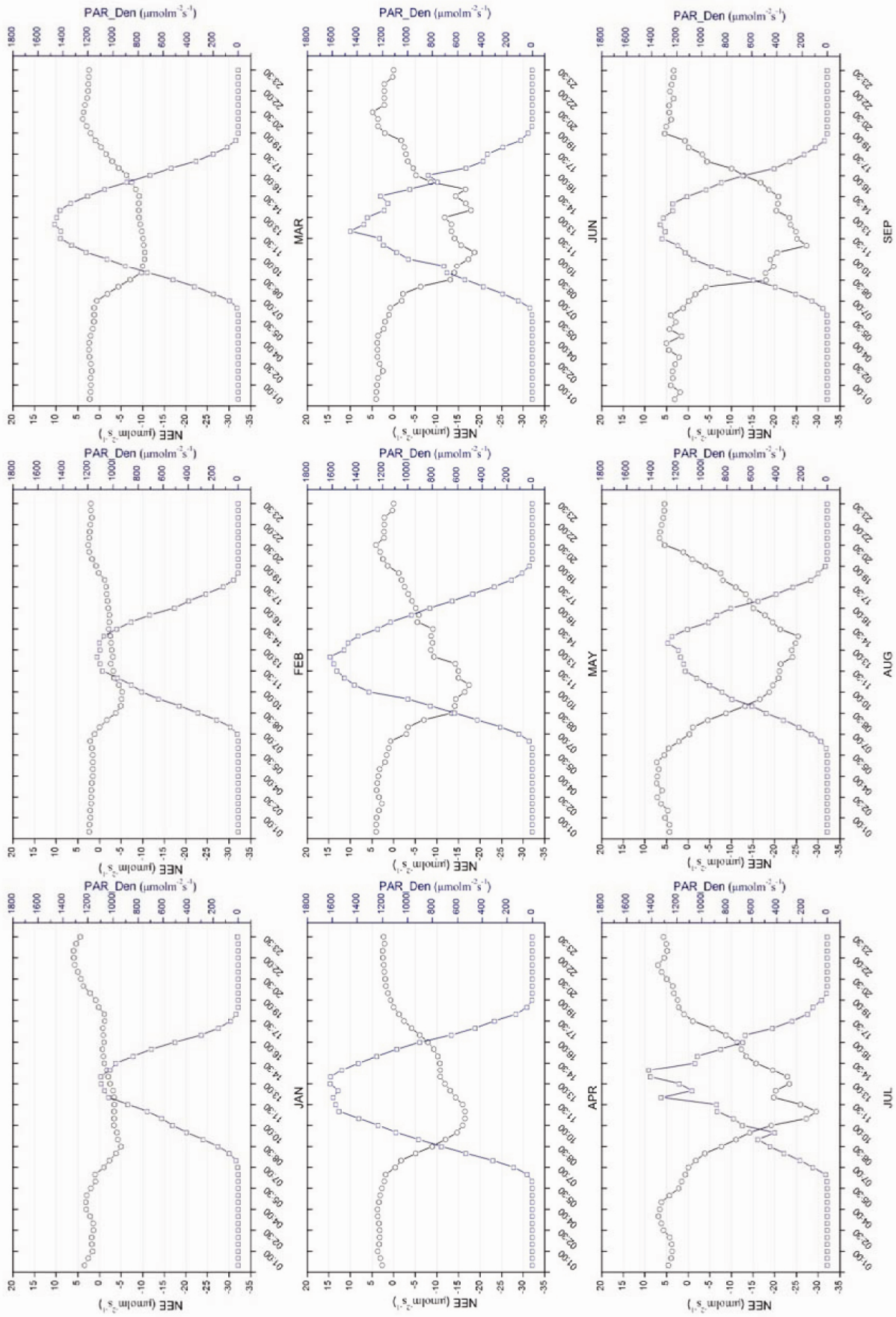


Figure 5. Mean monthly diurnal variation in NEE and PAR_den (photosynthetically active radiation density).

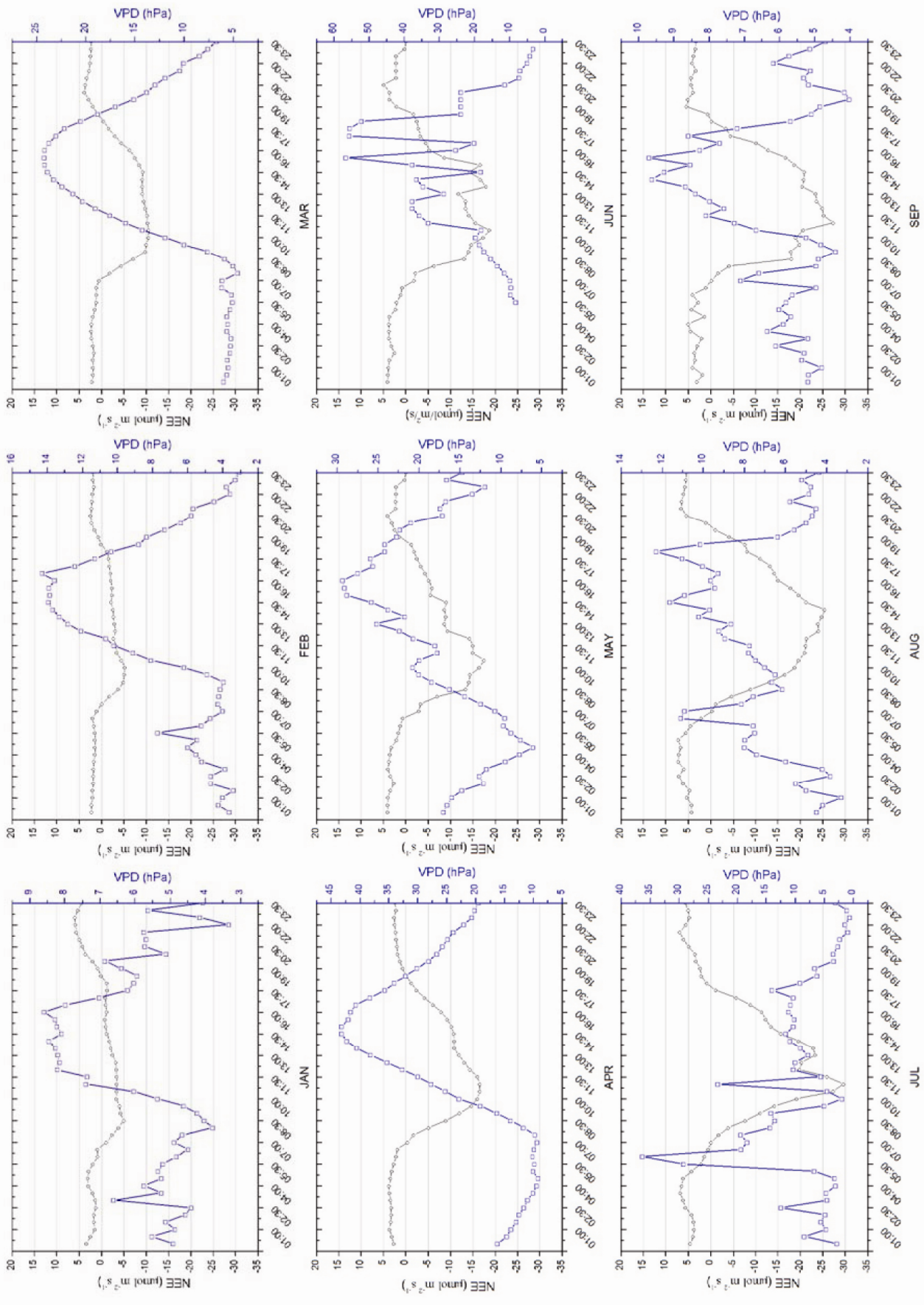


Figure 6. Mean monthly diurnal variation of NEE and vapour pressure deficit at the site.

Table 3. Monthly ecosystem photosynthesis parameters

Month	α ($\mu\text{mol CO}_2 \mu\text{mol photon}^{-1}$)	P_{max} ($\mu\text{mol CO}_2 \text{m}^{-2} \text{s}^{-1}$)	R_e ($\mu\text{mol CO}_2 \text{m}^{-2} \text{s}^{-1}$)	R^2
January	0.0056	2.92	0.38	0.10
February	0.007	2.03	0.0035	0.26
March	0.036	17.32	3.00	0.88
April	0.019	32.05	1.95	0.84
May	0.017	23.27	0.194	0.53
June	0.0305	38.14	2.45	0.82
July	0.042	52.49	4.097	0.73
August	0.036	81.62	4.67	0.90
September	0.033	71.5	3.14	0.94

R^2 , Correlation coefficient; P_{max} , Maximum photosynthetic energy; R_e , Daytime ecosystem respiration; α , Ecosystem apparent quantum yield.

negative at sunrise and reached its peak when PAR intensity was highest. A study on *Prosopis juliflora* by Pathre *et al.*³⁸ indicated that vapour pressure deficit (VPD) plays critical role in causing midday depression in the net photosynthesis and stomatal conductance compared to temperature or photosynthetic photon flux density (PPFD). Figure 6 shows the diurnal monthly variation of VPD along with variation in NEE. High variation in the mean monthly VPD value was observed, the highest being from April to July due to increase in air temperature and reduction in soil moisture. The mean diurnal monthly air temperature at 10 m height and soil moisture at 15 cm depth are shown in Figure 2 *a* and *d* respectively.

Quantifying ecosystem-specific parameter values of gross photosynthesis light response curves assumes significance for evaluating carbon budgets and improvement of ecosystem models for large-area applications^{25,39}. The ecosystem parameters α , P_{max} and R_e are important for describing ecosystem photosynthetic activity and to determine the shape of the light response curve^{30,40,41}. Gross photosynthesis is often represented by a rectangular hyperbola function of incident PAR⁴², where there is a near-linear increase in productivity at low light levels and an asymptotic approach to maximum productivity at high light levels. The ecosystem photosynthetic parameters were estimated using the Michaelis–Menten equation²⁵

$$\text{NEE} = \frac{\alpha * \text{PAR} * P_{\text{max}}}{\alpha * \text{PAR} + P_{\text{max}}} - R_e, \quad (2)$$

where α ($\mu\text{mol C } \mu\text{mol photon}^{-1}$) is the ecosystem apparent quantum yield, P_{max} ($\mu\text{mol C m}^{-2} \text{s}^{-1}$) the maximum photosynthetic capacity and R_e ($\mu\text{mol C m}^{-2} \text{s}^{-1}$) is the daytime ecosystem respiration. In the present study the influence of PAR on NEE was examined using rectangular hyperbolic function (eq. (2)). The coefficients of fitted rectangular hyperbolic relationship interpreted as ecosystem parameters and values are shown in Table 3. Results depict monthly variation in values of α , P_{max} and R_e for mixed plantation. In earlier months of the year, i.e. January and February, the α value remained very low but it

rose to a considerably high value in March (i.e. $0.036 \mu\text{mol C } \mu\text{mol photon}^{-1}$). In April, despite the high canopy cover, the α value reduced markedly due to desiccating effect of high VPD stress. The highest and lowest values of α were noticed in July and April respectively. In general, the higher value of α persisted during monsoon season (July to September) than summer because of lowering of VPD stress resulting from high soil moisture availability in subtropical monsoonal climate⁴¹. The highest value of α noticed in September reveals existence of the most favourable environmental conditions controlling photosynthesis and plant growth.

The value of P_{max} showed an increasing trend from March to August with advancement in canopy growth and rise in air temperature, except in May. P_{max} showed a dip in May and this was mainly attributed to adverse effect of extreme air temperature of 37.8°C recorded during this month. Daytime ecosystem respiration, R_e , was found to be very low in February ($0.0035 \mu\text{mol cm}^{-2} \text{s}^{-1}$) due to the leafless condition and small bole size. Canopy images captured using Phenocam camera clearly showed the phase of leaf formation from March to May in a year. Even though the favourable condition of higher air temperature and canopy cover existed, the low values of R_e observed during pre-monsoon months (i.e. March to May) could be better explained by limiting effect of soil moisture on ecosystem respiration. The high magnitude of R_e during June and July was due to positive effect of favourable environmental and biophysical factors such as temperature, soil moisture and optimal green biomass condition in the plantation ecosystem. Towards the end of active growing season, i.e. September, the R_e value again declined due to comparatively lower levels of soil moisture and air temperature conditions. On the other hand, strong correlation found between PAR and NEE during these months reflects better ecosystem light utilization efficiency under optimal temperature and canopy cover condition.

The present study highlights the role of EC technique in monitoring carbon dioxide and water vapour exchange over a mixed forest plantation in subtropical India. Diurnal

variation in carbon and water vapour fluxes over mixed forest plantation appeared to be more closely linked to driving forces such as radiation and VPD. However, the seasonal dynamics was largely influenced by phenology and soil moisture conditions resulting from subtropical monsoon climate. From the present study, we conclude that 9-year-old young mixed forest plantation is currently acting as a strong sink of carbon. Further, our findings on ecosystem parameters (α , P_{\max} and R_e) reflect the dominant role of phenology and environmental factors such as soil moisture and temperature. The monthly variations of ecosystem α and P_{\max} at the site were predominantly determined by the soil moisture and phenology. Information on these ecosystem parameters would have strong implication on improving models of ecosystem-level carbon cycling. The derived α , P_{\max} and R_e can be adopted in light use efficiency (LUE) and other process-based models such as EC-LUE, BIOME-BCG, LPJ etc. Though mixed plantation in the Terai Central Forest Division appeared to be a sink of carbon during 2013, it is imperative to plan long-term monitoring of carbon fluxes for determining the carbon source and sink nature of the site. Studies^{43,44} have reported several uncertainties in EC method for the assessment of the absolute values of the long-term net carbon exchange even in well-established sites, despite the ideal topography. Our experience was also similar. Power failed on some days in winter due to fog. For smooth running of the EC equipment, available wireless technology can be adopted for data download and equipment functioning monitoring. More EC towers in different phytogeographic zones of India, long-term flux monitoring, forest inventory and use of remote sensing and GIS can be effective in the upscaling of EC data over large areas.

1. Schlesinger, W. H., *Biogeochemistry: An Analysis of Global Change*, Academic Press, New York, 1991.
2. Chhabra, A. and Dadhwal, V. K., Estimating terrestrial net primary productivity over India using satellite data. *Curr. Sci.*, 2004, **86**(2), 269–271.
3. Calvo, E. and Jochem, E. (eds), IPCC Special Report on Carbon Dioxide Capture and Storage, Cambridge University Press, Cambridge, 2005.
4. Bachelet, D., Neilson, R. P., Lenihan, J. M. and Drapek, R. J., Climate change effects on vegetation distribution and carbon budget in the United States. *Ecosystems*, 2001, **4**, 164–185.
5. King, A. W. *et al.* (eds), US Climate Change Science Program, *The First State of the Carbon Cycle Report (SOCCR): The North American Carbon Budget and Implications for the Global Carbon Cycle*, Washington, DC, 2007.
6. Xiao, J. *et al.*, Twentieth century droughts and their impacts on terrestrial carbon cycling in China. *Earth Inter.*, 2009, **13**(10), 1–31.
7. Butler, M. P., Davis, K. J., Denning, A. S. and Kawa, S. R., Using continental observations in global atmospheric inversions of CO₂: North American carbon sources and sinks. *Tellus, Ser. B*, 2010, **62**, 550–572.
8. Barford, C. C. *et al.*, Factors controlling long- and short-term sequestration of atmospheric CO₂ in a mid-latitude forest. *Science*, 2001, **294**, 1688–1691.
9. Turner, D. P., Koerber, G. J., Harmon, M. E. and Lee, J. J., A carbon budget for forests of the conterminous United States. *Ecol. Appl.*, 1995, **5**, 421–436.
10. McGuire, A. D. *et al.*, Carbon balance of the terrestrial biosphere in the twentieth century: analysis of CO₂, climate and land use effects with four process-based ecosystem models. *Global Biogeochem. Cycles*, 2001, **15**, 183–206.
11. Baldocchi, D. D., Valentini, R., Running, S., Oechel, W. and Dahlen, R., Strategies for measuring and modeling carbon dioxide and water vapour fluxes over terrestrial ecosystems. *Global Change Biol.*, 1996, **2**, 159–168.
12. Goulden, M. L., Munger, J. W., Fan, S. M., Daube, B. C. and Wofsy, S. C., Measurements of carbon sequestration by long-term eddy-covariance: methods and a critical evaluation of accuracy. *Global Change Biol.*, 1996, **2**, 169–182.
13. Goulden, M. L. *et al.*, Sensitivity of boreal forest carbon balance to soil thaw. *Science*, 1998, **279**, 214–217.
14. Baldocchi, D. D. and Meyers, T. P., On using eco-physiological, micrometeorological and biogeochemical theory to evaluate carbon dioxide, water vapor and trace gas fluxes over vegetation: a perspective. *Agric. For. Meteorol.*, 1998, **90**, 1–25.
15. Baldocchi, D. D. *et al.*, FLUXNET: a new tool to study the temporal and spatial variability of ecosystem-scale carbon dioxide, water vapor, and energy flux densities. *Bull. Am. Meteorol. Soc.*, 2001, **82**, 2415–2434.
16. Dadhwal, V. K., Kushwaha, S. P. S., Patel, N. R. and Yogesh, K., Carbon flux monitoring in India. *ENVIS For. Bull.*, 2010, **9**(2), 46–49.
17. Patel, N. R., Dadhwal, V. K. and Saha, S. K., Measurement and scaling of carbon dioxide (CO₂) exchange in wheat using flux-tower and remote sensing. *J. Indian Soc. Remote Sensing*, 2011, **39**(3), 383–391.
18. Andrew, J. O., Terrestrial ecosystem-atmosphere exchange of water and energy from FLUXNET: review and meta analysis of a global *in-situ* observatory. *Geogr. Compass*, 2012, **6**(12), 689–705.
19. Sundareswar, P. V. *et al.*, Environmental monitoring network for India. *Science*, 2007, **316**(5822), 204–205.
20. Xiao, J. *et al.*, Estimation of net ecosystem carbon exchange of the conterminous United States by combining MODIS and AmeriFlux data. *Agric. For. Meteorol.*, 2008, **148**, 1827–1847.
21. Anon., Management Plan for Terai Central Forest Division (1999–2000 to 2008–2009). Working Plan Circle, Nainital, 1999, pp. 33–42.
22. Burba, G., *Eddy Covariance Method for Scientific, Industrial, Agricultural, and Regulatory Applications: A Field Book on Measuring Ecosystem Gas Exchange and Areal Emission Rates*, LI-COR Biosciences, Lincoln, NE, USA, 2013, p. 331.
23. Lee, X., On micrometeorological observations of surface-air exchange over tall vegetation. *Agric. For. Meteorol.*, 1998, **91**, 39–49.
24. Baldocchi, D. D., Finnigan, J., Wilson, K. B., Paw, U. K. and Falge, E., On measuring net ecosystem carbon exchange over tall vegetation on complex terrain. *Bound.-Layer Meteorol.*, 2000, **96**, 257–291.
25. Falge, E. *et al.*, Gap filling strategies for defensible annual sums of net ecosystem exchange. *Agric. For. Meteorol.*, 2001, **107**, 43–69.
26. Reichstein, M. *et al.*, On the separation of net ecosystem exchange into assimilation and ecosystem respiration: review and improved algorithm. *Global Change Biol.*, 2005, **11**, 1424–1439.
27. Anderson, D. E., Verma, S. B. and Rosenberg, N. J., Eddy correlation measurements of CO₂, latent heat and sensible heat fluxes over a crop surface. *Bound.-Layer Meteorol.*, 1984, **29**, 263–272.
28. Verma, S. B., Baldocchi, D. D., Anderson, D. E., Matt, D. R. and Clement, R. J., Eddy fluxes of CO₂, water vapor, and sensible heat over a deciduous forest. *Bound.-Layer Meteorol.*, 1986, **36**, 71–91.
29. Mahr, L., Flux sampling errors for aircraft and towers. *J. Atmos. Ocean. Technol.*, 1998, **15**, 416–429.
30. Hollinger, D. Y., Goltz, S. M., Davidson, E. A., Lee, J. T., Tu, K. and Valentine, H. T., Seasonal patterns and environmental control

of carbon dioxide and water vapour exchange in an ecotonal boreal forest. *Global Change Biol.*, 1999, **5**, 891–902.

31. Anthoni, P., Law, B. E. and Unsworth, M. J., Carbon and water vapor exchange of an open-canopied ponderosa pine ecosystem. *Agric. For. Meteorol.*, 1999, **95**, 151–168.
32. Schmid, H. P., Grimmond, C. S. B., Cropley, F., Offerle, B. and Su, H. B., Measurements of CO₂ and energy fluxes over a mixed hardwood forest in the mid-western United States. *Agric. For. Meteorol.*, 2000, **103**, 357–374.
33. Collatz, G. J., Ball, J. T., Grivet, C. and Berry, J. A., Regulation of stomatal conductance and transpiration: a physiological model of canopy processes. *Agric. For. Meteorol.*, 1991, **54**, 107–136.
34. Stannard, D. I., Blanford, J. H., Kustas, W. P., Nichols, W. D., Amer, S. A., Schmugge, T. J. and Weltz, M. A., Interpretation of surface flux measurements in heterogeneous terrain during the Monsoon'90 experiment. *Water Resour. Res.*, 1994, **30**(5), 1227–1239.
35. Twine, T. E. *et al.*, Correcting eddy-covariance flux underestimates over a grassland. *Agric. For. Meteorol.*, 2000, **103**, 279–300.
36. Jarvis, P. G. and Leverenz, J. W., Productivity of temperate, deciduous and evergreen forests In *Encyclopaedia of Plant Physiology, New Series* (eds Lange, O. L. *et al.*), Springer-Verlag, Berlin, 1983, vol. 12D, pp. 233–280.
37. Haszpra, L., Barea, Z., Davis, K. J. and Tarczay, K., Long-term tall tower carbon dioxide flux monitoring over an area of mixed vegetation. *Agric. For. Meteorol.*, 2005, **132**, 58–77.
38. Pathre, U. V., Sinha, A. K., Shirke, P. A. and Sane, P. V., Factors determining the mid-day depression of photosynthesis in trees under monsoon climate. *Trees*, 1998, **12**, 472–481.
39. Gilmanov, T. G., Verma, S. B., Sims, P. L., Meyers, T. P., Bradford, J. A., Burba, G. G. and Suyker, A. E., Gross primary production and light response parameters of four Southern Plains ecosystems estimated using long-term CO₂-flux tower measurements. *Global Biogeochem. Cycle*, 2003, **17**(2), 1071.
40. Ruimy, A., Javis, P. G., Baldocchi, D. D. and Saugier, B., CO₂ fluxes over plant canopies and solar radiation: a review. *Adv. Ecol. Res.*, 1995, **26**, 1–69.
41. Zhang, L. M. *et al.*, Seasonal variations of ecosystem apparent quantum yield (α) and maximum photosynthesis rate (P_{max}) of different forest ecosystems in China. *Agric. For. Meteorol.*, 2006, **137**, 176–187.
42. Thornley, J. H. M. and Johnson, I. R., *Plant and Crop Modelling: A Mathematical Approach to Plant and Crop Physiology*, Clarendon, Oxford, England, 1990, p. 669.
43. Massman, W. J. and Lee, X. H., Eddy-covariance flux corrections and uncertainties in long-term studies of carbon and energy exchanges. *Agric. For. Meteorol.*, 2002, **113**, 121–144.
44. Baldocchi, D. D., Assessing ecosystem carbon balance: problems and prospects of the eddy-covariance technique. *Global Change Biol.*, 2003, **9**, 478–492.

ACKNOWLEDGEMENTS. This study was carried out under the National Carbon Project (NCP) funded by ISRO Geosphere Biosphere Programme. We thank the Forest Department, Uttarakhand for permission to set up the flux tower; Dr B. S. Burfal (former Principal Chief Conservator of Forests and Head of Forest Force), Dr R. B. S. Rawat (Principal Chief Conservator of Forests and Head of Forest Force), Mrs Veena Sekri (Principal Chief Conservator of Forests), Mr A. R. Sinha (Addl. Principal Chief Conservator of Forests), Mr Jairaj (Addl. Principal Chief Conservator of Forests) and Dr Parag M. Dhakate (Deputy Conservator of Forests, Terai Central Forest Division, Haldwani) for continuous support during this study. T.W., S.P.S.K. and N.R.P. thank Dr Y. V. N. Krishna Murthy (Director, Indian Institute of Remote Sensing) for providing the necessary facilities during this study.

Received 25 March 2014; revised accepted 25 June 2014

Assessment and monitoring of deforestation from 1930 to 2011 in Andhra Pradesh, India using remote sensing and collateral data

P. Hari Krishna, K. R. L. Saranya*, C. Sudhakar Reddy, C. S. Jha and V. K. Dadhwal

National Remote Sensing Centre, ISRO, Balanagar, Hyderabad 500 037, India

Deforestation is one of the greatest threats to the world's forest ecosystems. The present study has utilized remote sensing and GIS techniques to quantify changes in forest cover and to map patterns of deforestation in Andhra Pradesh, India during 1930–2011. Andhra Pradesh has the second largest recorded forest area and ranks sixth with an actual forest cover amongst all Indian states. Forest cover maps from seven temporal datasets were prepared based on interpretation of multi-source topographical maps and satellite data. A representative set of landscape indices has been used to study landscape-level changes over time. The mapping for the period of 1930, 1960, 1975, 1985, 1995, 2005 and 2011 indicates that the forest cover accounts for 85,392, 68,063, 46,940, 45,520, 44,409, 43,577 and 43,523 sq. km of the study area respectively. The study found the net forest cover declined as 49% of the total forest area during the last eight decades. The annual rate of estimated deforestation during 2005–2011 was 0.02%. Annual rate of deforestation of teak mixed forests was relatively higher (0.76) followed by mangroves (0.58%), semi-evergreen forests (0.43%), dry deciduous forests (0.21%), moist deciduous forests (0.09%) and dry evergreen forests (0.07%) during 1975–2011. The landscape analysis shows that the number of forest patches was 3,981 in 1930, 5,553 in 1960, 8,760 in 1975, 9,412 in 1985, 9,646 in 1995 and 10,597 in 2011, which indicates ongoing anthropogenic pressure on the forests. The mean patch size (sq. km) of forest decreased from 21.5 in 1930 to 12.3 in 1960 and reached 3.9 by 2011. The analysis of historical forest cover changes provides a basis for management effectiveness and future research on various components of biodiversity, climate change and accounting of carbon.

Keywords: Collateral data, deforestation, landscape metrics, remote sensing.

THERE is increasing attention on the protection of tropical forests for the future of mankind¹. Deforestation has been identified as the primary threat for loss of biodiversity², responsible for 18% of global carbon dioxide emissions, impacts on climate³ and livelihoods of people dependent on forests⁴. Deforestation is defined as an event in a

*For correspondence. (e-mail: saranyakotturu@gmail.com)